Inorganic Chemistry

Article

pubs.acs.org/IC

(α-DT-TTF)$_2$[Au(mnt)$_2$]: A Weakly Disordered Molecular Spin-Ladder System

Rafaela A. L. Silva,[†] Ana I. S. Neves,[†] Elsa B. Lopes,[†] Isabel C. Santos,[†,§] Joana T. Coutinho,[†] Laura C. J. Pereira,[†] Concepció Rovira,[‡] Manuel Almeida,*[,†] and Dulce Belo*[,†]

[†]Department of Chemistry, IST/ITN, Instituto Superior Técnico, Universidade Técnica de Lisboa/CFMCUL, Estrada Nacional 10, P-2686-953 Sacavém, Portugal

[‡]Institut de Ciencia de Materials de Barcelona (ICMAB-CSIC) and CIBER-BBN, Campus UAB, E-08193 Bellaterra, Spain

[§]Centro de Química Estrutural, Instituto Superior Técnico, Universidade Técnica de Lisboa, P-1049-001 Lisboa, Portugal

Supporting Information

ABSTRACT: The synthesis and characterization of (α-DT-TTF)$_2$[Au(mnt)$_2$] is reported. The magnetic properties of this new salt show that it is still a rare example of an organic spin-ladder. (α-DT-TTF)$_2$[Au(mnt)$_2$] shares the same ladder structure of the DT-TTF and ETT-TTF analogues, and its room temperature conductivity is ~2 S/cm. Despite the observed donor orientation disorder associated with the thiophenic sulfur atoms, the intermolecular interactions between donor units, calculated using the extended Hückel approximation and a double-ξ basis set, show that the interaction values do not depend on the configuration of the sulfur atom on the thiophenic ring. The insensitivity of the spin-ladder magnetic properties to the donor molecular disorder in (α-DT-TTF)$_2$[Au(mnt)$_2$] is a direct consequence of the negligible contribution of the disordered thiophenic sulfur atom to the HOMO. In the related donor ETT-TTF, this contribution is significant and destroys the magnetic interactions, and no spin-ladder is observed. This compound not only enlarges the number of organic spin-ladder systems in this series of closely related compounds but also provides an interesting example of weakly disordered molecular spin-ladder system.

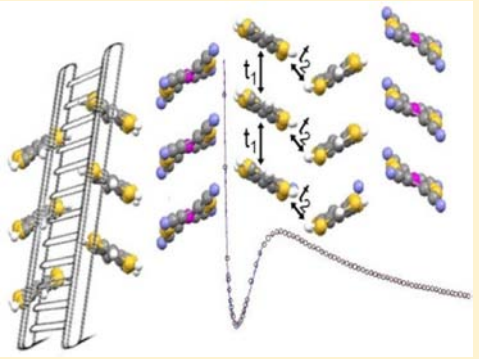

INTRODUCTION

Spin-ladders are magnetic systems, composed of a finite number of coupled spins chains in a situation that is intermediate between the purely 1D system of isolated chains and 2D system of planes. The spin-ladders have attracted particular interest during the last two decades due to quantum effects which, depending on the specific topology, e.g., the number of legs (interacting chains), can lead to a significantly different magnetic behavior, with a gap in the magnetic excitations for an even number of chains, while the ladders with an odd number of chains are gap-less.[1] The interest in these systems has been also stimulated by the exciting prediction that doped ladders can become superconducting due to an effective attraction between holes in chains mediated by magnetic interactions.[1a,b,2]

Following our report of the first organic based molecular spin-ladder system (DT-TTF)$_2$[Au(mnt)$_2$] (DT-TTF = dithiophenetetrathiafulvalene; mnt = maleonitriledithiolate),[3] different attempts were explored in order to achieve related spin-ladder systems, which could provide important structure–properties correlations, by chemical means of simple molecular modifications, on both the donor and acceptor components. The possible molecular changes of the donors which could preserve the ladder structure and specific spin-ladder behavior proved however to be rather limited. There is a large number of diamagnetic anionic metal-bisdithiolenes closely related to [Au(mnt)$_2$], with different ligands and metals that can be used. However, it was found that the replacement of the anions in (DT-TTF)$_2$[Au(mnt)$_2$] by species other than those based on the ligand mnt or *i*-mnt (*i*-mnt = 1,1-dicyanoethylene-2,2-dithiolate) leads to completely different crystal structures.[4] The number of available donors related with DT-TTF is much smaller than the anions. So far, concerning changes on the donor side, only the replacement of the DT-TTF donor by ETT-TTF (ETT-TTF = ethylenethiophenetetrathiafulvalene, Scheme 1) could preserve the ladder structure of the original (DT-TTF)$_2$[Au(mnt)$_2$] compound, but the orientation disorder of the ETT-TTF asymmetric donor completely destroyed

Scheme 1. Chemical Structures of ETT-TTF, DT-TTF, and α-DT-TTF

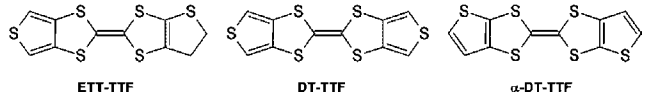

Received: January 31, 2013
Published: April 5, 2013

   dx.doi.org/10.1021/ic400246y | *Inorg. Chem.* 2013, 52, 5300–5306

the magnetic spin-ladder behavior.[5] The number of molecular spin-ladder compounds is still relatively small,[6] and until the present these based on derivatives of $(DT\text{-}TTF)_2[Au(mnt)_2]$ provided the only series of closely related spin-ladder systems.[5]

In this Article, we explore charge-transfer compounds based on the related donor α-DT-TTF (α-DT-TTF = alpha-dithiophenetetrathiafulvalene) that TTF that previously has been very poorly explored, until our recent report of its full characterization,[7] and describe in detail the compound $(\alpha\text{-}DT\text{-}TTF)_2[Au(mnt)_2]$. This compound shares the same structure type of $(DT\text{-}TTF)_2[Au(mnt)_2]$ with donors arranged in paired stacks. Notably, the magnetic properties of a spin-ladder system are preserved in spite of the orientation disorder of the donor; therefore, this compound provides an interesting example of a weakly disordered spin-ladder system at variance with the ETT-TTF analogue which behaved as a strongly disordered ladder system.

RESULTS AND DISCUSSION

Crystals of $(\alpha\text{-}DT\text{-}TTF)_2[Au(mnt)_2]$ were obtained by electrocrystallization of α-DT-TTF in the presence of a tetrabutylammonium salt of $[Au(mnt)_2]$ in dichloromethane solution, over platinum electrodes using standard galvanostatic conditions, after about 3 days. Similar attempts to obtain crystals with analogous anions $[M(mnt)_2]^-$, with other metals M = Pt, Ni, and Cu lead at variance with the DT-TTF donor, to completely different structures and stoichiometries. This is due to the lower oxidation potential of the α-DT-TTF donor with respect to DT-TTF[7] which tends to form more easily fully ionic salts and may reduce the anions to the dianions. With M = Ni, two structures with stoichiometries $(\alpha\text{-}DT\text{-}TTF^+)_2[Ni(mnt)_2]^{2-}$ and $(\alpha\text{-}DT\text{-}TTF)^+[Ni(mnt)_2]^-$ were obtained, both with fully oxidized donors. The first compound with a 2:1 stoichiometry is formed by a spontaneous redox reaction upon mixing the neutral donor with the monoanion $[Ni(mnt)_2]^-$. The compound with a 1:1 stoichiometry is obtained upon electrocrystallization of the solution resulting from the first reaction. The crystal structures of these two compounds were solved by single crystal diffraction and are presented in detail as Supporting Information. With M = Pt and Cu, similar compounds are obtained under the same conditions; however, we have only been able to solve the crystal structure of $(\alpha\text{-}DT\text{-}TTF^+)_2[Pt(mnt)_2]^{2-}$. This structure is of a different type and is also presented as Supporting Information. The formation of charge transfer salts with fully oxidized donors is not unprecedented among thiophene-TTF type donors, which due to their low oxidation potential when combined with $[M(mnt)_2]^-$ often leads to its reduction to a dianion.[5,8]

On the other hand, $(\alpha\text{-}DT\text{-}TTF)_2[Au(mnt)_2]$ crystallizes in the monoclinic space group $P2_1/n$ and is so far the only example of a salt of this donor that is isostructural with $(DT\text{-}TTF)_2[Au(mnt)_2]$. Crystal and structural refinement data are listed in Table 1.

The asymmetric unit is composed of one α-DT-TTF donor molecule (Figure 1 and Table 2) and half $[Au(mnt)_2]^-$ anion with the gold atom placed in an inversion center (Figure 2 and Table 3). Both units are essentially planar. A relevant feature of this structure is that the α-DT-TTF donors are disordered, with both ends of the molecule presenting the thiophenic sulfur atoms in two possible positions with occupation factors of ∼0.5 (Table 2).

Although the possibility of cis−trans disorder cannot be excluded from X-rays, this disorder results most probably from the orientation disorder of the donors which are obtained primarily in the most stable trans-configuration.[7]

Table 1. Crystal and Refinement Data for $(\alpha\text{-}DT\text{-}TTF)_2[Au(mnt)_2]$[a]

	$(\alpha\text{-}DT\text{-}TTF)_2[Au(mnt)_2]$
formula	$C_{28}H_8AuN_4S_{16}$
molecular mass	1110.31
T (K)	150
dimensions (mm^3)	0.2 × 0.03 × 0.02
cryst color	golden brown
cryst syst	monoclinic
space group	$P2_1/n$
a (Å)	16.2482(18)
b (Å)	3.8807(4)
c (Å)	26.958(3)
β (deg)	100.419(4)
V (Å^3)	1671.8(3)
Z	2
ρ_{calcd} (g cm^{-3})	2.206
intervals h, k, l	±19, ±4, −23/+32
$2\theta_{max}$ (deg)	23.99
reflns collected	8479
indep reflns	3159
reflns > $2\sigma(I)$	2177
R1	0.04
wR2	0.07

[a]Crystallographic data (excluding structure factors) was deposited with the Cambridge Crystallographic Data Centre with no. CCDC 91655.

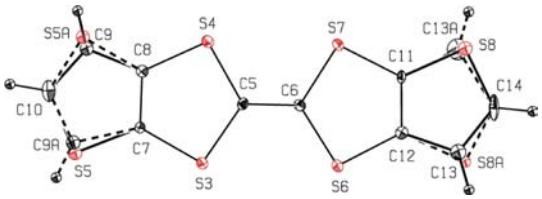

Figure 1. ORTEP view of $(\alpha\text{-}DT\text{-}TTF)^{0.5+}$ with disorder model and with atom numbering scheme, in the crystal structure of $(\alpha\text{-}DT\text{-}TTF)_2[Au(mnt)_2]$.

In spite of this disorder the α-DT-TTF donor units are arranged in pairs of stacks related by a screw axis (Figure 3) as in $(DT\text{-}TTF)_2[Au(mnt)_2]$.

The interplanar distances between donor molecules (3.557 Å) are comparable to those found in the DT-TTF salts, and the two donor stacks are connected by very short S···S contacts at 3.466 Å as shown in Figure 3. A relevant difference between these two salts is the absence of significant short contact between pairs of donor chains in the α-DT-TTF compound due to the absence of a terminal sulfur atom in this donor. Therefore, the paired chains are expected to behave as more isolated in the α-DT-TTF salt.

In this structure there are three types of intermolecular donor−donor interactions: t_1, between donors along the chains; t_2, between molecules in nearby paired chains; and t_3, between molecules in different pairs of chains (Figures 3 and 4). These interactions between neighboring donor units can be estimated by calculations based on the extended Hückel approximation using a double-ξ basis, which predict a HOMO as shown in Figure 5. In spite of the uncertainty of the absolute values obtained by the theoretical calculations under this approach,

dx.doi.org/10.1021/ic400246y | Inorg. Chem. 2013, 52, 5300−5306

Table 2. Intramolecular Bond Distances of $[\alpha\text{-DT-TTF}]^{0.5+}$ in the Crystal Structure of $(\alpha\text{-DT-TTF})_2[Au(mnt)_2]$

	d (Å)
S3−C5	1.747(7)
S3−C7	1.731(8)
S4−C8	1.743(7)
S4−C5	1.751(6)
S5−C7	1.694(8)
S5−C10	1.637(9)
S5A−C10	1.569(14)
S5A−C8	1.660(13)
S6−C6	1.743(6)
S6−C12	1.743(7)
S7−C6	1.751(7)
S7−C11	1.736(8)
S8−C11	1.687(8)
S8−C14	1.613(10)
S8A−C14	1.499(13)
S8A−C12	1.706(13)
C5−C6	1.373(9)
C7−C8	1.379(9)
C7−C9A	1.66(5)
C8−C9	1.446(17)
C9−C10	1.385(18)
C9A−C10	1.38(5)
C11−C12	1.367(11)
C11−C13A	1.53(5)
C12−C13	1.448(18)
C13−C14	1.382(18)
C13A−C14	1.66(5)
C9−H9	0.9504
C9A−H9A	0.9451
C10−H10	0.9501
C13−H13	0.9508
C13A−H13A	0.9395
C14−H14	0.9496

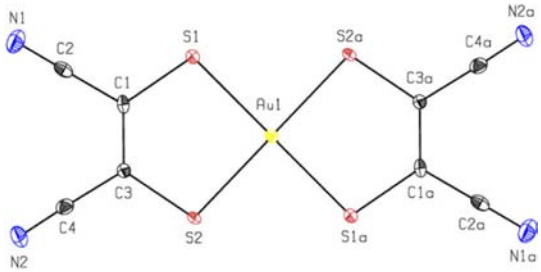

Figure 2. ORTEP view of $[Au(mnt)_2]^-$ with atom numbering scheme, in the crystal structure of $(\alpha\text{-DT-TTF})_2[Au(mnt)_2]$.

the results provide an accurate relative comparison between the α-DT-TTF, ETT-TTF, and the DT-TTF salts.

In the α-DT-TTF salt due to the possible cis/trans and orientation disorder of donors one has to consider all the possible configurations between the donor pairs. As schematically depicted in Figure 4 for the first type of interaction t_1, there are 7 possible pair configurations: 2 trans/trans, 3 cis/cis, and 2 cis/trans. The values calculated for the three types of interactions t_1, t_2, and t_3 in $(DT\text{-}TTF)_2[Au(mnt)_2]$ and the corresponding ones in $(\alpha\text{-DT-TTF})_2[Au(mnt)_2]$, which are split in the 7 possible configurations, are listed in Table 4 .

Table 3. Intramolecular Bond Distances of $[Au(mnt)_2]^-$ in the Crystal Structure of $(\alpha\text{-DT-TTF})_2[Au(mnt)_2]$

	d (Å)
Au1−S1	2.3151(19)
Au1−S2	2.3165(19)
S1−C1	1.746(7)
S2−C3	1.752(6)
C1−C2	1.429(11)
C1−C3	1.353(10)
C3−C4	1.431(11)
N2−C4	1.133(11)
N1−C2	1.142(11)

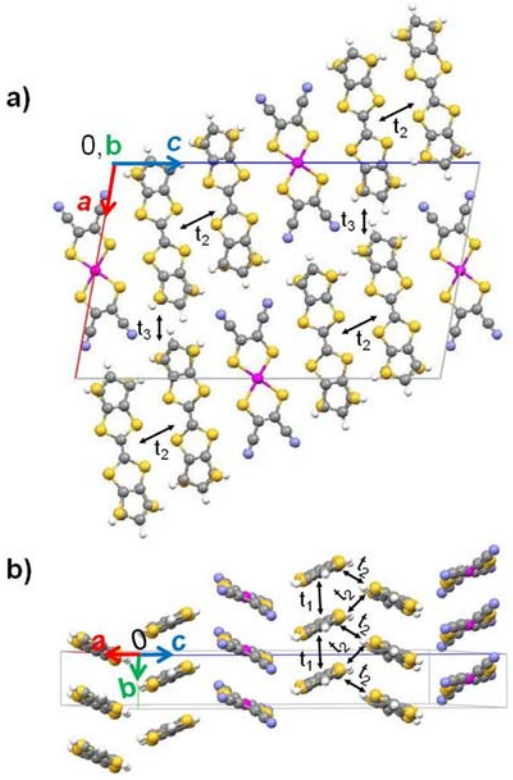

Figure 3. Crystal structure of $(\alpha\text{-DT-TTF})_2[Au(mnt)_2]$ with indication of relevant interdonor interactions: (a) viewed along the *b*-axis; (b) partial view showing one layer of neighboring donor and acceptor stacks.

As it can be seen in Table 4 these interaction values do not significantly depend on the pair configuration. This is due to the negligible electronic density of the HOMO in the thiophenic sulfur atoms. Therefore, the disorder of the thiophenic groups in α-DT-TTF, 50% in two possible orientations, is expected to have a relatively soft effect in the electronic properties of its salts. This situation contrasts with ETT-TTF in which the HOMO has a considerable electronic density in the disordered thiophenic sulfur atom (Figure 5).

The comparison between the interaction calculated for the two salts $(\alpha\text{-DT-TTF})_2[Au(mnt)_2]$ and $(DT\text{-}TTF)_2[Au(mnt)_2]$ shows that the former presents a slightly smaller interaction t_1 along the chains, a larger interaction t_2 between chains in a pair, and a smaller interaction t_3 between chains of different pairs. This last interaction was already found to be small and magnetically irrelevant in the DT-TTF salts.[3,9]

dx.doi.org/10.1021/ic400246y | Inorg. Chem. 2013, 52, 5300−5306

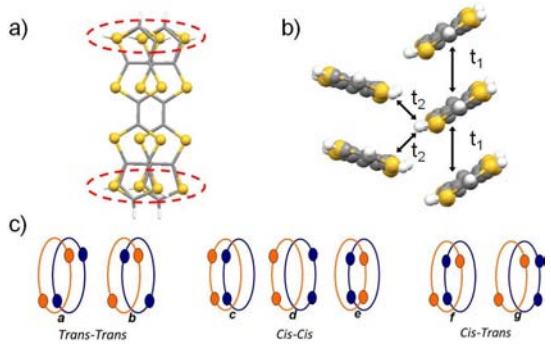

Figure 4. (a) Donor–donor overlap mode in $(\alpha\text{-DT-TTF})_2[Au(mnt)_2]$ showing the disorder in thiophenic S atom; (b) schematic representation of the interactions t_1 and t_2 in the crystal structure of α-DT-TTF; (c) schematic representation of 7 possible configurations between the donor pairs where the circles indicate the S atom position in the thiophenic ring.

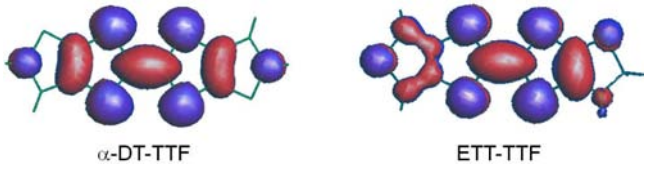

Figure 5. Schematic representation of the HOMO of α-DT-TTF and ETT-TTF.

Table 4. Intermolecular Interactions t_1, t_2, t_3 (meV) between Donor Units Calculated Using the Extended Hückel Approximation and a Double-ξ Basis Set in $(\alpha\text{-DT-TTF})_2[Au(mnt)_2]$ and $(DT\text{-TTF})_2[Au(mnt)_2]$[a]

	t_1	t_2	t_3
trans–trans $(\alpha\text{-DT-TTF})_2[Au(mnt)]_2$	a, 52.1; b, 46.0	a, 77.6; b, 74.3	a, 4.0; b, 4.0
cis–cis $(\alpha\text{-DTTTF})_2[Au(mnt)]_2$	c, 49.4; d, 56.6; e, 47.2	c, 77.0; d, 74.1; e, 74.1	c, 5.4; d, 3.7; e, 3.7
cis–trans $(\alpha\text{-DT-TTF})_2[Au(mnt)]_2$	f, 59.2; g, 44.7	f, 73.9; g, 73.9	f, 4.0; g, 2.0
$(DT\text{-TTF})_2[Au(mnt)]_2$	104.6	66.3	15.3

[a]In the first compound the three type of contacts are split in 7 possible different pair configurations, a–g, which are identified in Figure 4.

The electrical transport properties of $(\alpha\text{-DT-TTF})_2[Au(mnt)_2]$ were studied by conductivity and thermoelectric power measurements in single crystals along their long axis (chain axis b of the crystal structure), and results are shown in Figures 6 and 7 in comparison with those of the related $(DT\text{-TTF})_2[M(mnt)_2]$ salts. The electrical conductivity of $(\alpha\text{-DT-TTF})_2[Au(mnt)_2]$ at room temperature is ~2 S/cm, significantly smaller than in the DT-TTF salts (10–50 S/cm), and with clear semiconducting regime corresponding to an activation energy of 36 meV (Figure 6). The reduced electrical conductivity is consistent with slightly smaller intermolecular interactions along the chain axis, and in addition, the electronic localized semiconducting behavior with higher activation energy can be also enhanced by some disorder effects.

Thermoelectric power results with values of ~25 μV/K at room temperature, decreasing upon cooling and crossing zero at ~230 K, are consistent with the semiconducting behavior shown by conductivity measurements (Figure 7).

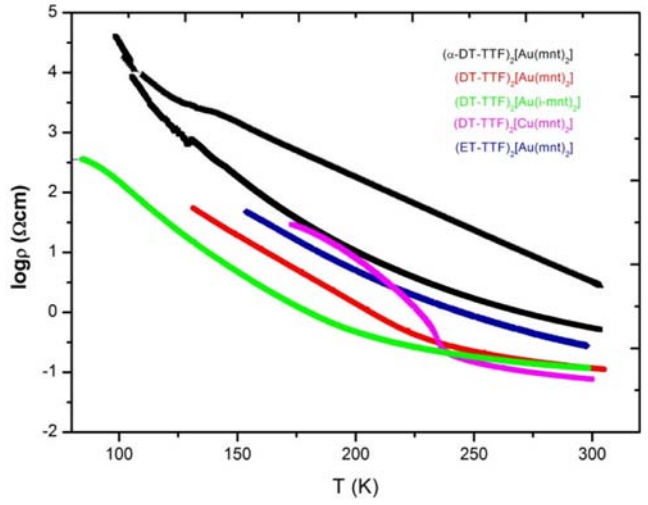

Figure 6. Electrical resistivity of $(\alpha\text{-DT-TTF})_2[Au(mnt)_2]$ and related compounds as a function of temperature.

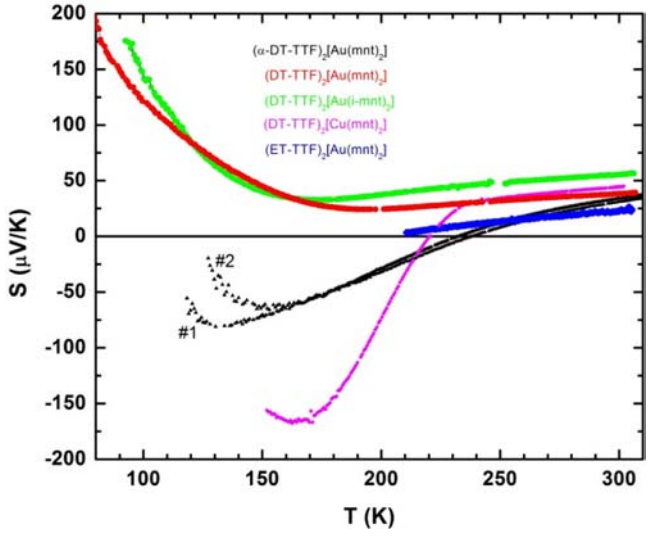

Figure 7. Thermoelectric power of $(\alpha\text{-DT-TTF})_2[Au(mnt)_2]$ and related compounds as a function of temperature.

In view of the electronic localization shown by transport measurements, and considering that each two donors carry a spin, it is of obvious interest to investigate the magnetic susceptibility and characterize a possible spin-ladder behavior in this compound.

The paramagnetic susceptibility, χ_p, obtained from static (SQUID) magnetization measurements measured in the range 2–300 K considering a correction of core diamagnetism is shown in Figure 8. Upon cooling, there is a broad maximum in the susceptibility at ca. 70 K followed by an exponential decrease which at lower temperatures is overcome, below 10 K, by a dominating Curie-like tail corresponding to approximately 3% $S = {}^1/_2$ spins. In the high-temperature region ($T > 100$ K) the magnetic susceptibility shows a Curie–Weiss behavior with a negative Weiss temperature, $\theta = -62$ K, demonstrating the presence of dominant AFM interactions. This behavior, with localized spins interacting antiferromagnetically and displaying a gap in the spin excitations at low temperatures, is close to that observed in other previous reported spin-ladder compounds[4,5]

dx.doi.org/10.1021/ic400246y | Inorg. Chem. 2013, 52, 5300–5306

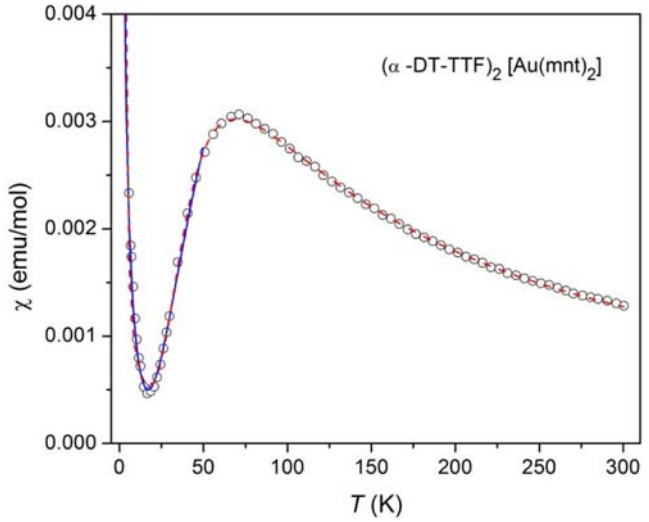

Figure 8. Static paramagnetic susceptibility, χ_p, of $(\alpha$-DT-TTF$)_2$[Au(mnt)$_2$] as a function of temperature T. Full line and dashed line correspond to the models of Troyer[10] and Barnes and Riera[11] fits for T < 50 K and 4−300 K, respectively. This last model fitting data gives values of $J_\perp$ = 100 and $J_\parallel$ = 54 K.

and comparable to (DT-TTF)$_2$[M(mnt)$_2$] with M = Au and Cu.[3a,5]

Following an approach comparable to that used in similar molecular spin-ladder compounds the magnetic susceptibility data was fitted considering two components, a major contribution due to the spin-ladders, χ_{ladder}, and a minor Curie component, χ_{Curie}, which takes into account possible magnetic defects and impurities.

$$\chi = f\chi_{ladder} + (1 - f)\chi_{Curie} \quad (1)$$

Here, f is the molar fraction. The ladder contribution can be estimated following two approaches. At lower temperatures it can be estimated using the spin-ladder model given by Troyer et al.,[10] for a two-legged spin-ladder system

$$\chi_{ladder} = \alpha T^{-1/2} \exp(-\Delta/kT) \quad (2)$$

where α is a constant corresponding to the dispersion of the excitation energy, and Δ is the finite energy gap in the spin-excitation spectrum given by[10a]

$$\Delta_{spin} \approx J_\perp - J_\parallel + \frac{J_\parallel^2}{2J_\perp} \quad (3)$$

$J_\perp$ and $J_\parallel$ are the interactions between spins along the ladder rails and the rungs, respectively. A rather good fit of the low temperature data below 50 K was obtained with this equation with parameters f = 0.96 and Δ_{spin} = 70 K.

As alternative approach to the ladder contribution enabling to deduce both exchange coupling constants, $J_\perp$ and $J_\parallel$, is given by the two-legged ladder model of Barnes and Riera[11] which can be used to fit the experimental data in temperature range 4−300 K:

$$\chi_{ladder} = \frac{c_1}{T}\left[1 + \left(\frac{T}{c_2}\right)^{c_3}(e^{c_4/T} - 1)\right]^{-1}\left[1 + \left(\frac{c_5}{T}\right)^{c_6}\right]^{-1} \quad (4)$$

Here the coefficients $c_1 = Ng^2\mu_B{}^2/4k_B$ and c_2, c_3, c_4, c_5, and c_6 are function of the exchange constants $J_\perp$ and $J_\parallel$.

As shown in Figure 8, both equations can fit our data accurately, with this last model fitting data in the extended range of temperature 4−300 K (dotted line) with $J_\perp$ = 100 and $J_\parallel$ = 54 K. Although the obtained ratio $J_\perp/J_\parallel$ =1.85 is slightly out of the limits 0.9 < $J_\perp/J_\parallel$ < 1.1 defined by Barnes and Riera for an ideal spin-ladder,[11] it agrees qualitatively with the ratio of the transfer integrals evaluated when the dimeric nature of the elementary building block of the spin-ladder has been taken into account. Considering the situation $J_\perp > J_\parallel$ of the theoretical model of Troyer et al.,[10] the spin gap and the coupling values were calculated from the combination of eq 3 with the following quadratic expression[10]

$$T(\chi_{max})/J_\perp = 0.625 - 0.01835\frac{J_\parallel}{J_\perp} + 0.2532\left(\frac{J_\parallel}{J_\perp}\right)^2 \quad (5)$$

giving values of $J_\perp$ = 100.14(1.26) K and $J_\parallel$ = 54.13(2.60) K. The spin gap calculated with these coupling constants, Δ_{spin} = 68 K, is only slightly lower than the value determined with eq 2 but still in good agreement.

These values should be compared with those obtained for related compounds with the same structure type: (DT-TTF)$_2$[M(mnt)$_2$] with M = Au and Cu and (DT-TTF)$_2$[Au(*i*-mnt)$_2$], shown in Table 5. It is worth noting that the larger $J_\perp$ and smaller $J_\parallel$ values observed in $(\alpha$-DT-TTF$)_2$[Au(mnt)$_2$] when compared with the (DT-TTF)$_2$[Au(mnt)$_2$] spin-ladder systems are well correlated with the changes of the electronic interaction parameters estimated from Hückel calculations shown in Table 4.

Table 5. Spin-Ladder Interaction Parameters in Thiophene-TTF Type Compounds

compd	$J_\perp$ (K)	$J_\parallel$ (K)	Δ (K)	ref
$(\alpha$-DT-TTF$)_2$[Au(mnt)]$_2$	100	54	68	this work
(DT-TTF)$_2$[Au(mnt)]$_2$	142	82	78	3
			83[a]	
(DT-TTF)$_2$[Cu(mnt)]$_2$	218	121	130.6[a]	5
(DT-TTF)$_2$[Au(*i*-mnt)]$_2$	142	86	82[a]	5

[a]From single crystal EPR data.

One-dimensional fermion systems like spin chains are known to be extremely sensitive to disorder. The disorder effects in spin-ladders may be however quite different depending on its nature. The relative insensitivity of the spin-ladder magnetic properties of $(\alpha$-DT-TTF$)_2$[Au(mnt)$_2$] to the donor orientation disorder, at variance with the case of (ETT-TTF)$_2$[Au(mnt)$_2$], is a direct consequence of the HOMO geometry. Therefore, $(\alpha$-DT-TTF$)_2$[Au(mnt)$_2$] exemplifies a theoretically predicted situation[12] of weak magnetic disorder in a spin-ladder system, while the (ETT-TTF)$_2$[Au(mnt)$_2$] compound with the same structural orientation disorder exemplifies a strong magnetic disorder situation that destroys the spin-ladder behavior.

CONCLUSIONS

In conclusion, among several salts based on the recently explored donor α-DT-TTF with [M(mnt)$_2$] anions with different transition metals the gold salt $(\alpha$-DT-TTF$)_2$[Au(mnt)$_2$] is the only one sharing the same ladder structure of the DT-TTF analogue, and in spite of the donor cis−trans/orientation disorder associated with the thiophenic sulfur atoms, it presents a spin-ladder magnetic behavior. The relative

dx.doi.org/10.1021/ic400246y | Inorg. Chem. 2013, 52, 5300−5306

insensitivity of the spin-ladder magnetic properties to the molecular orientation disorder in this compound is a direct consequence of the negligible contribution of the disordered thiophenic sulfur atoms to the HOMO of this donor, at variance with ETT-TTF analogue where this contribution is significant. Therefore, not only does this compound enlarge the number of spin-ladder systems in this series of closely related compounds, which so far remain the only such series of isostructural molecular organic spin-ladder systems, but it also provides an interesting example of weakly disordered molecular spin-ladder system.

EXPERIMENTAL SECTION

Synthesis of (α-DT-TTF)$_2$[Au(mnt)$_2$]. Crystals were obtained by electrocrystallization. A dichloromethane solution of the donor and the acceptor salt, in approximately stoichiometric amounts, was added to the H-shaped cell, with Pt electrodes and in galvanostatic conditions. The tetrabuthylammonium salt of $[Au(mnt)_2]^-$ was synthesized and purified by recrystallization as previously described.[13] Dichloromethane was also purified using standard procedures and freshly distilled immediately before its use. The system was sealed under nitrogen and after ~3 days, using a current density of 1 μA cm^{-2}, and brown plate-shaped crystals were collected in the anode and washed with dichloromethane. Anal. Calcd for $AuC_{28}H_8N_4S_{16}$: C 30.29, H 0.73, N 5.05, S 46.20. Found: C 30.01, H 0.70, N 4.96, S 46.12%.

Electrical Transport Properties. Electrical conductivity and thermopower measurements in single crystals were performed in the temperature range 50−320 K, using a measurement cell attached to the cold stage of a closed cycle helium refrigerator. In the first step, the thermopower was measured by using a slow ac (ca. 10−2 Hz) technique,[14] by attaching two 25 μm diameter 99.99% pure Au wires (Goodfellow metals), thermally anchored to two quartz reservoirs, with Pt pain (Demetron 308A) to the extremities of an elongated sample as in a previously described apparatus,[15] controlled by a computer.[16] The oscillating thermal gradient was kept below 1 K and was measured with a differential Au-0.05 at. % Fe versus chromel thermocouple of the same type. The absolute thermoelectric power of the sample was obtained after correction for the absolute thermopower of the Au leads, by using the data of Huebner.[17]

Magnetic Measurements. The magnetic susceptibility was measured with a S700X SQUID magnetometer (Cryogenic Ltd.) in the temperature range 2−300 K, assuming a diamagnetic contribution of 4.2×10^{-4} emu mol^{-1} (estimated from tabulated Pascal constants)

X-ray Diffraction Studies. Experiments were performed with a Bruker AXS APEX CCD detector diffractometer using graphite monochromated Mo Kα radiation (λ = 0.710 73 Å), in the φ and ω scans mode. A semiempirical absorption correction was carried out using SADABS.[18] Data collection, cell refinement, and data reduction were done with the SMART and SAINT programs.[19] The structures were solved by direct methods using SIR97[20] and refined by full-matrix least-squares methods using the program SHELXL97[21] using the winGX software package.[22] Non-hydrogen atoms were refined with anisotropic thermal parameters whereas H-atoms were placed in idealized positions and allowed to refine riding on the parent C atom. Molecular graphics were prepared using ORTEP 3.[23]

Intermolecular Energy Interactions Calculations. The interaction energies were calculated[24] by employing the extended Hückel method.[25] The basis set consisted of Slater type orbitals of double-ζ quality. The exponents, contraction coefficients, and atomic parameters were taken from previous work.[26]

ASSOCIATED CONTENT

Supporting Information

Figures and crystal structure description of the related compounds (α-DT-TTF)$_2$[Ni(mnt)$_2$], (α-DT-TTF)$_2$[Pt(mnt)$_2$], and (α-DT-TTF)[Ni(mnt)$_2$]. Table of the short contacts in the crystal structure of (α-DT-TTF)$_2$[Au(mnt)$_2$]. This material is available free of charge via the Internet at http://pubs.acs.org.

AUTHOR INFORMATION

Corresponding Author

*E-mail: dbelo@ctn.ist.utl.pt (D.B.); malmeida@ctn.ist.utl.pt (M.A.).

Notes

The authors declare no competing financial interest.

ACKNOWLEDGMENTS

This work was supported by FCT (Portugal) through Contracts PTDC/QUI-QUI/101788/2008 and PTDC/QEQ-SUP/1413/2012 and by DGI, Spain (Contract CTQ2010-195011/BQU), the Generalitat de Catalunya (2009SGR00516), the CIBER de Bioingeniera, Biomateriales y Nanomedicina (CIBER-BBN), promoted by ISCIII, Spain. It also benefited from COST action D35.

ABBREVIATIONS

ET-TTF, ethylenethiophenetetrathiafulvalene; mnt, maleonitriledithiolate; i-mnt, 1,1-dicyanoethylene-2,2-dithiolate; α-DT-TTF, alpha-dithiophenetetrathiafulvalene

REFERENCES

(1) (a) Dagotto, E.; Rice, T. M. Rice *Science* **1996**, *271*, 618. (b) Scalapino, D. J. *Nature* **1995**, *377*, 12. (c) Hiroi, Z.; Takano, M. *Nature* **1995**, *337*, 41. (d) Azuma, M.; Hiroi, Z.; Tanako, M.; Ishida, K.; Kitaoka, I. *Phys. Rev. Lett.* **1994**, *73*, 3463.

(2) (a) Dagotto, E.; Riera, J.; Scalapino, D. J. *Phys. Rev. B* **1992**, *45*, 5744. (b) Goplan, S.; Rice, T. M.; Sigrist, M. *Phys. Rev. B* **1994**, *49*, 8901. (c) Barnes, T.; Riera, J. *Phys. Rev. B* **1994**, *49*, 6819. (d) White, S. R.; Noack, R. M.; Scalapino, D. J. *Phys. Rev. Lett.* **1994**, *73*, 882. (e) Hayword, C. A.; Poiblanc, D.; Levy, L. P. *Phys. Rev. Lett.* **1995**, *75*, 926.

(3) (a) Rovira, C.; Veciana, J.; Ribera, E.; Tarres, J.; Canadell, E.; Rousseau, R.; Mas, M.; Molins, E.; Almeida, M.; Henriques, R. T.; Morgado, J.; Schoeffel, J.-P.; Pouget, J.-P. *Angew. Chem., Int. Ed.* **1997**, *36*, 2324. (b) Ribera, E.; Rovira, C.; Veciana, J.; Tarrés, J.; Canadell, E.; Rousseau, R.; Molins, E.; Mas, M.; Schoeffel, J.-P.; Pouget, J.-P.; Morgado, J.; Henriques, R. T.; Almeida, M. *Chem.−Eur. J.* **1999**, *5*, 2025.

(4) Dias, J. C.; Ribas, X.; Morgado, J.; Seiça, J.; Lopes, E. B.; Santos, I. C.; Henriques, R. T.; Almeida, M.; Wurst, K.; Foury-Leylekian, P.; Canadell, E.; Vidal-Gancedo, J.; Veciana, J.; Rovira, C. *J. Mater. Chem.* **2005**, *15*, 3187.

(5) Ribas, X.; Mas-Torrent, M.; Pérez-Benítez, A.; Dias, J. C.; Alves, H.; Lopes, E. B.; Henriques, R. T.; Molins, E.; Santos, I. C.; Wurst, K.; Foury-Leylekian, P.; Almeida, M.; Veciana, J.; Rovira, C. *Adv. Funct. Mater.* **2005**, *15*, 1023.

(6) (a) Rovira, C. *Structure and Bonding (Berlin)*; Springer-Verlag: Berlin, Germany, 2001; Vol. *100*, pp 163−188. (b) Fourmigue, M. *Acc. Chem. Res.* **2004**, *37*, 179. (c) Clay, R. T.; Mazmudar, S. *Phys. Rev. Lett.* **2005**, *94*, 207206.

(7) Silva, R. A. L.; Neves, A. I. S.; Afonso, M. L.; Santos, I. C.; Lopes, E. B.; Del Pozo, F.; Pfattner, R.; Maas, M.; Rovira, C.; Almeida, M.; Belo, D. *Eur. J. Inorg. Chem.*, DOI: 10.1002/ejic.201201362.

(8) (a) Silva, R. A. L.; Afonso, M. L.; Santos, I. C.; Belo, D.; Freitas, R. R.; Lopes, E. B.; Coutinho, J. T.; Pereira, L. C. J.; Henriques, R. T.; Almeida, M.; Rovira, C. *Phys. Status Solidi C* **2012**, *9*, 1134. (b) Rovira, C.; Pérez-Benítez, A.; Molins, E.; Mata, I.; Almeida, M.; Alves, H.; Veciana, J.; Gama, V.; Lopes, E. B.; Henriques, R. T. *Synth. Met.* **2003**, *133*, 523. (c) Mas-Torrent, M.; Alves, H.; Lopes, E. B.; Almeida, M.; Wurst, K.; Vidal-Gancedo, J.; Veciana, J.; Rovira, C. *J. Solid State Chem.* **2002**, *168*, 563. (d) Mas-Torrent, M. Ph.D. Thesis. Univ. Autonoma de Barcelona, Spain, 2002.

(9) Arcon, D.; Lappas, A.; Margadonna, S.; Prassides, K.; Ribera, E.; Veciana, J.; Rovira, C.; Henriques, R. T.; Almeida, M. *Phys. Rev. B* **1999**, *60*, 4191.
(10) (a) Troyer, M.; Tsunetsugu, H.; Würtz, D. *Phys. Rev. B* **1994**, *50*, 13515. (b) Troyer, M.; Zhitomirsky, M. E.; Ueda, K. *Phys. Rev. B* **1997**, *55*, 6117.
(11) (a) Barnes, T.; Riera, J. *Phys. Rev. B* **1994**, *49*, 68179. (b) Barnes, T.; Dagotto, E.; Riera, J.; Swanson, E. S. *Phys. Rev. B* **1993**, *47*, 3196.
(12) (a) Orignac, E.; Giamarchi, T. *Phys. Rev. B* **1998**, *57*, 5811. (b) Mélin, R.; Lin, Y.-C.; Lajkó, P.; Rieger, H.; Iglói, F. *Phys. Rev. B* **2002**, *65*, 104415.
(13) Werden, B. G.; Billig, E.; Gray, H. B. *Inorg. Chem.* **1966**, *5*, 78.
(14) Chaikin, P. M.; Kwak, J. F. *Rev. Sci. Instrum.* **1975**, *46*, 218.
(15) Almeida, M.; Oostra, S.; Alcácer, L. *Phys. Rev. B* **1984**, *30*, 2839.
(16) Lopes, E. B. INETI-Sacavém, Internal Report, Portugal 1991.
(17) Huebner, R. P. *Phys. Rev. A* **1964**, *135*, 1281.
(18) Sheldrick, G. M. *SADABS*; Bruker AXS Inc.: Madison, WI, 2004.
(19) *SMART and SAINT*; Bruker AXS Inc.: Madison, WI, 2004.
(20) Altomare, A.; Burla, M. C.; Camalli, M.; Cascarano, G.; Giacovazzo, G.; Guagliardi, A.; Moliterni, A. G. G.; Polidori, G.; Spagna, R. *J. Appl. Crystallogr.* **1999**, *32*, 115.
(21) Sheldrick, G. M. *SHELXL97, Program for Crystal Structure Refinement*; University of Göttingen: Germany, 1997.
(22) Farrugia, L. J. *J. Appl. Crystallogr.* **1999**, *32*, 837.
(23) Farrugia, L. J. *J. Appl. Crystallogr.* **1997**, *30*, 565.
(24) Ren, J.; Liang, W.; Whangbo, M.-H.*Crystal and Electronic Structure Analysis Using CAESAR*; PrimeColor Software, Inc.: Cary, North Carolina, 1998.
(25) (a) Hoffmannn, R. *J. Chem. Phys.* **1963**, *39*, 1397. (b) Whangbo, M.-H.; Hoffmannn, R. *J. Am. Chem. Soc.* **1978**, *100*, 6093.
(26) Canadell, E.; Rachidi, I.E.-I.; Ravy, S.; Pouget, J. P.; Brossard, L.; Legros, J. P. *J. Phys. (Paris)* **1989**, *50*, 2967.